EPJ Web of Conferences **17**, 16015 (2011)
DOI: 10.1051/epjconf/20111716015

Effects of the valence neutron of the lithium isotopes in ^{6,7,8}Li+^{208}Pb systems

Su Youn Lee[1] and Woonyoung So[2,a]

[1] Department of Physics, Dong-Eui University, Busan 614-714, Korea
[2] Department of Radiological Science, Kangwon National University, Samcheok 245-711, Korea

Abstract. Using the measured experimental data for ^{6,7,8}Li+^{208}Pb system, we investigated the relation between the interaction distance and the lowest threshold separation energy of the projectiles. Although ^{6}Li can be considered more weakly bound projectile than ^{8}Li, the lithium isotope with the largest interaction distance is not ^{6}Li but ^{8}Li. Also, we can infer that the difference of the semiexperimental direct reaction (DR) cross sections and the total breakup / transfer reaction cross sections comes from α and ^{7}Li capture. Finally, the barrier height, V_B, of ^{8}Li + ^{208}Pb system compared with ^{7}Li + ^{208}Pb system are reduced about 3MeV. This is the rise of flux from the elastic into the reaction channel, which tends to enhance $\sigma_R^{\rm exp}$. As a result, we can deduce that the valence neutron play a role as the lowering of the barrier height.

1 Introduction

In our recent study [1], we carried out analyses based on the extended optical model [2,3], in which the optical potential consists of the energy independent Hartree-Fock part and the energy dependent complex polarization potential for the ^{6}Li + ^{208}Pb and ^{7}Li + ^{208}Pb systems. In Ref. [1], using such an extended optical potential, we performed the simultaneous χ^2 analyses of the elastic scattering and fusion cross section data, determining the two components of the polarization potentials as functions of the incident energy.

In the present work, we will investigate the characteristic features of the heavy ion reaction for the lithium isotopes including ^{8}Li. The unstable radioactive nucleus ^{8}Li is a loosely bound nuclei, with a threshold separation energy S_n=2.033MeV (^{8}Li $\rightarrow$ ^{7}Li+n). The threshold separation energy of ^{8}Li is between those for ^{6}Li [S_α=1.475MeV (^{6}Li $\rightarrow$ α+d)] and ^{7}Li [S_α=2.468MeV (^{7}Li $\rightarrow$ α+t)]. This primary breakup channels, ^{8}Li $\rightarrow$ ^{7}Li+n, includes 1n-transfer and breakup processes producing ^{7}Li nuclei and one neutron. It is similar to the breakup process for neutron rich nuclei such as ^{6}He and ^{11}Be. From consecutive breakup process of ^{7}Li nuclei (^{7}Li $\rightarrow$ α+t), however, an additional α-particle yield can be observed [4]. At near and below Coulomb-barrier energies, therefore, the large transfer and breakup cross sections for ^{8}Li+^{208}Pb system have been measured in Ref. [4]. As shown in Table. 1, indeed, the total reaction cross section is dominated by the DR cross section including the transfer and the breakup cross sections. According to the dominant DR cross section, therefore, we can expect that the complete fusion (CF) suppression takes place at above Coulomb-barrier [5]. In order to investigate this suppression, we study precisely the effect of the breakup on the fusion for ^{8}Li+^{208}Pb system.

In Sec. 2, we will first explain the so-called semiexperimental total reaction cross sections, $\sigma_R^{\rm semi\text{-}exp}$, from the elastic scattering, and then will obtain the semiexperimental DR cross sections, $\sigma_D^{\rm semi\text{-}exp}$ from Eq. (2) using the fusion cross section data. In Sec. 3, we will analyses the experimental cross section data for lithium isotopes. In addition, we discuss the relation between the interaction distance and the lowest threshold separation energy of the projectiles and the distinction of the total reaction cross section for lithium isotopes. Also, we will examine the role of the valence neutron(s) on the the barrier height. Section 4 concludes the paper.

2 Extracting semiexperimental DR and total reaction cross sections

To carry out the present study, we have first to extract the semiexperimental total reaction cross sections, $\sigma_R^{\rm semi\text{-}exp}$, denoted as

$$\sigma_R^{\rm semi\text{-}exp} = \sigma_C - \sigma_E, \qquad (1)$$

which can be extracted from the measured elastic scattering cross sections, $d\sigma_E/d\Omega$, in heavy-ion collisions [6,7]. Here σ_C and σ_E are the angle-integrated total Rutherford and elastic scattering cross sections, respectively. Note that the semiexperimental total reaction cross sections are defined as the sum of all the non elastic integrated cross sections including the inelastic cross sections.

Equation (1) is based on the optical theorem for charged particles [6], which reads $\sigma_R^{\rm semi\text{-}exp} = \sigma_C$ - σ_E + $\Delta\sigma$. Here

[a] e-mail: wyso@kangwon.ac.kr

Table 1. The measured complete fusion cross sections and the extracted DR and total reaction cross sections. $\sigma_R^{\text{semi-exp}}$ (in mb) are extracted from the measured elastic scattering cross sections and $\sigma_D^{\text{semi-exp}}$ are taken from Eq. (2). Here, σ_F^{exp} for ^{6}Li+^{208}Pb, ^{7}Li+^{208}Pb, and ^{8}Li+^{208}Pb are taken from Refs. [5,8,9]. Note that the experimental data for ^{7}Li+^{208}Pb are replaced by those for ^{7}Li+^{209}Bi because we have no available experimental data.

System	$E_{c.m.}$ (MeV)	σ_F^{exp} (mb)	$\sigma_D^{\text{semi-exp}}$ (mb)	$\sigma_R^{\text{semi-exp}}$ (mb)
^{6}Li+^{208}Pb	28.2	22	206	228
	30.1	120	311	431
	32.1	234	432	666
	34.0	335	562	897
	37.9	507	796	1303
^{7}Li+^{208}Pb	28.1	18	120	138
	30.0	88	239	327
	31.9	218	354	572
	33.9	366	421	787
	37.7	650	592	1242
	42.6	866	687	1553
^{8}Li+^{208}Pb	24.4	0.3†	224.7	225
	27.6	10†	494	504
	28.9	36†	588	624
	30.6	128†	757	885
	33.1	327	892	1219

† These values are extrapolated from Eq. (3).

$\Delta\sigma$ is given in terms of the nuclear part of the forward scattering amplitude, $f^N(\theta)$ =0, as $\Delta\sigma = 4\pi/k$ Im $[f^N(\theta)]$. For heavy ion collisions, $\Delta\sigma$ is generally small, justifying the use of Eq. (4) for generating $\sigma_R^{\text{semi-exp}}$.

Once $\sigma_R^{\text{semi-exp}}$ is extracted, and if the experimental fusion cross section, σ_F^{exp}, is available, one can further generate a semiexperimental DR cross section, $\sigma_D^{\text{semi-exp}}$, as

$$\sigma_D^{\text{semi-exp}} = \sigma_R^{\text{semi-exp}} - \sigma_F^{\text{exp}}. \quad (2)$$

The measured complete fusion cross sections and the extracted DR and total reaction cross sections for ^{6,7,8}Li + ^{208}Pb systems are listed in Table 1. For the ^{6}Li + ^{208}Pb system, since the cross sections σ_F^{exp} obtained from Ref. [8] fluctuate with respect to the incident energies, we extracted their experimental cross sections using Wong's formula,

$$\sigma(E) = \frac{R_B^2\hbar\omega}{2E_{c.m.}} \ln\left\{1 + \exp\left[\frac{2\pi}{\hbar\omega}(E_{c.m.} - V_B)\right]\right\}, \quad (3)$$

as the measured fusion cross sections. Here, V_B, $\hbar\omega$, and R_B are the Coulomb barrier energy, the barrier curvature, and the interaction radius, respectively [10].

Table 2 shows these parameters for the complete fusion cross sections of lithium isotopes incident on ^{208}Pb and ^{209}Bi. Figure 1 shows the complete fusion are shown as functions of (a) $E_{c.m.}$ and (b) $E_{c.m.} - V_B$ for ^{6,8,9}Li + ^{208}Pb and ^{6,7}Li + ^{209}Bi systems. We can see that the complete fusion data are nearly the same shape. As seen in Fig. 1 (b), particulary, such feature can best be seen as functions of $E_{c.m.} - V_B$. At high energy $E_{c.m.} \approx$ 37.7MeV, however, the values of σ_F^{exp} for ^{6}Li + ^{208}Pb system deviate from those of σ_F^{exp} for ^{7}Li + ^{208}Pb system by about 30%.

Table 2. The Coulomb barrier parameters for the complete fusion cross sections of lithium isotopes incident on ^{208}Pb and ^{209}Bi. The Coulomb barrier parameters for the complete fusion for are extracted by using Wong's formula, Eq. (3).

System	V_B	$\hbar\omega$	R
^{6}Li+^{208}Pb	29.3	6.06	8.79
^{6}Li+^{209}Bi	29.7	6.28	8.62
^{7}Li+^{209}Bi	29.3	5.36	9.33
^{8}Li+^{208}Pb	29.1	7.00	9.35
^{9}Li+^{208}Pb	28.5	5.63	9.62

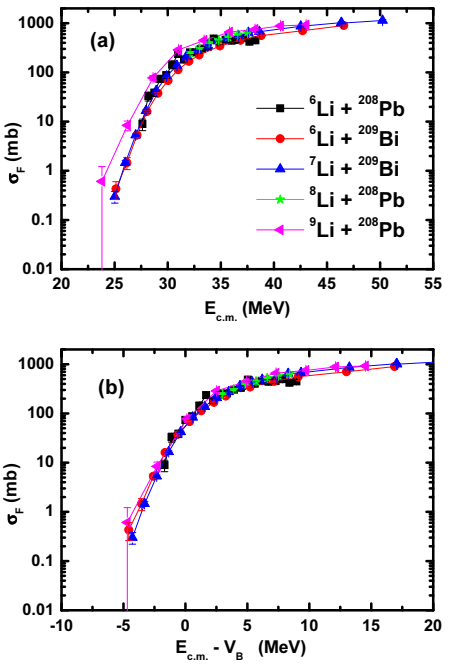

Fig. 1. (Color online) The complete fusion cross section, σ_F, are shown as functions of (a) $E_{c.m.}$ and (b) $E_{c.m.} - V_B$ for ^{6}Li+^{208}Pb [8], ^{6,7}Li+^{209}Bi [9], ^{8}Li+^{208}Pb [5], and ^{9}Li+^{208}Pb [11] systems.

3 Analyses of the experimental cross section data for lithium isotopes

In this paper, one of the characteristic features for the experimental cross section data is the relation between the interaction distance and the lowest threshold separation energy of the projectiles. In order to discuss this relation, we define the ratio, P_E, given as

$$P_E \equiv \frac{d\sigma_{el}}{d\sigma_\Omega} \Big/ \frac{d\sigma_C}{d\sigma_\Omega} = \frac{d\sigma_{el}}{d\sigma_C} \quad (4)$$

as a function of the distance of the closest approach D (or the reduced distance d), where $d\sigma_{el}/d\sigma_\Omega$ and $d\sigma_C/d\sigma_\Omega$

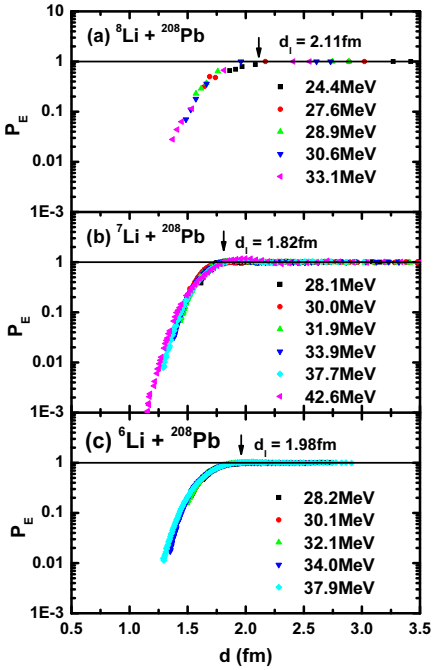

Fig. 2. (Color online) P_E values for (a) ^{8}Li+^{208}Pb system [4], (b) ^{7}Li+^{208}Pb system [12], and (c) ^{6}Li+^{208}Pb system [12].

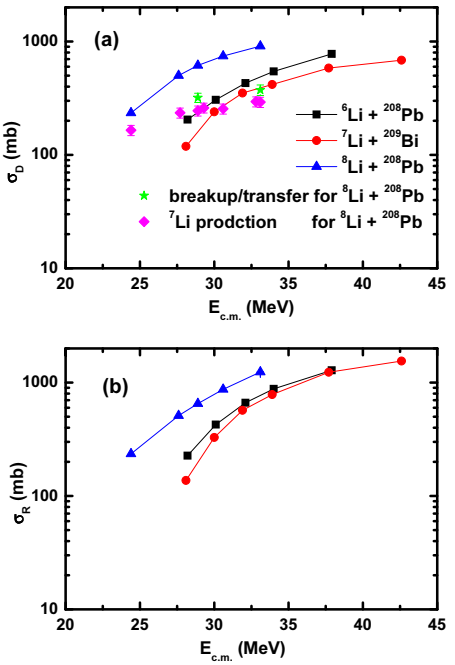

Fig. 3. (Color online) The (a) DR and (b) total reaction cross section, σ_D and σ_R, are shown as functions of $E_{c.m.}$ for ^{6,7,8}Li+^{208}Pb systems. These values are taken from Eq. (2). Also shown is the total transfer/breakup cross section (diamonds) as well as the ^{7}Li production cross sections (stars) for ^{8}Li+^{208}Pb system.

Table 3. The relation between the interaction distance and the lowest threshold separation energy (**Bold typeface**) of ^{6,7,8}Li projectiles.

	d_I (fm)	$S_{\rm n}$ (MeV)	$S_{\rm p}$ (MeV)	S_α (MeV)
^{6}Li+^{208}Pb	1.98	5.66	4.59	**1.47**
^{7}Li+^{208}Pb	1.82	7.25	9.98	**2.47**
^{8}Li+^{208}Pb	2.11	**2.03**	12.45	7.38

are the elastic and Coulomb scattering cross section, respectively [1].

Generally, the collision between the heavy nuclei near coulomb barrier energy, V_B, is governed by the Coulomb and nuclear forces. In the asymptotic region, where the nuclear forces do not reach, the projectile nuclei mainly move along the classical Coulomb scattering trajectory. Thus, P_E remains close to unity until two ions approach each other within interaction distance, d_I. The interaction distance is determined as the place at which the ratio P_E drops to 0.99. However, if the two nuclei come close on feeling sufficient nuclear force, the projectile particles due to the strong attractive nuclear force transfer direct reaction such as neutron transfer reaction, breakup reaction, and incomplete fusion, or complete fusion rather than the elastic scattering moving along the Coulomb scattering trajectory. Within d_I, as a result, P_E begins to fall off. Actually, the experimental values of P_E as a function of the reduced distance d for ^{6,7,8}Li+^{208}Pb systems are plotted on Fig. 2 and the resultant value of the interaction distance and the lowest α-particle or neutron threshold separation energy, S_i (i = n, or p, or α) are listed in table 3. From the point of view of the threshold separation energy, as seen in table 3, we can consider that ^{6}Li is the most characteristic weakly bound projectile, ^{8}Li is the next, ^{7}Li is the least among these three under consideration. Thus, we can predict that ^{6}Li has the larger interaction distance than ^{7,8}Li because it is more easily broken by the nuclear forces. As seen in Table. 3, however, lithium isotope with the largest interaction distance is not ^{6}Li but ^{8}Li. Although the threshold separation energy is lower, thus, the interaction distance is not always far. Another characteristic feature of the experimental data for lithium isotopes can be seen the distinction of the total reaction cross section including the fusion and DR cross sections. We found that the complete fusion cross sections are essentially independent for the considered lithium isotopes in Sec. 2. However, it is found that the DR and total reaction cross sections for lithium isotopes are related considerably to the projectiles from Fig. 3. As seen in Fig. 3 (a), the DR cross sections of ^{6}Li and ^{7}Li are slightly different. Thus, the total reaction cross sections of them are also not significantly different. But, the DR and total reaction cross sections of ^{6,7}Li and ^{8}Li are considerably distinct. In order to explain the difference of the DR and total reaction cross sections for ^{8}Li with respect to ^{6,7}Li, we will investigate to the contribution for the constituent of the DR cross sections and the Coulomb barrier for the total reaction cross sections.

Figure 3 (a) shows the total breakup / transfer cross sections as well as the ^{7}Li production cross sections. There are two processes which product ^{7}Li cluster in ^{8}Li+^{208}Pb reaction. one is the elastic breakup (EBU) process which any particles are not captured by the target. One ^{7}Li par-

Table 4. The same as in Table 2, but for the total reaction cross sections.

System	V_B	$\hbar\omega$	R
^{6}Li+^{208}Pb	27.8	9.95	12.45
^{7}Li+^{208}Pb	28.1	7.44	12.17
^{8}Li+^{208}Pb	24.9	11.40	12.25

ticles are measured at the EBU process, $^{8}\mathrm{Li} \rightarrow {}^{7}\mathrm{Li} + \mathrm{n}$. Another is the 1n-transfer process which a neutron is captured by the target after EBU process, so that one ^{7}Li particles are also measured. Thus, the ^{7}Li production cross sections denoted as the diamonds mean the sum of the elastic breakup cross (EBU) sections and 1n-transfer cross sections, $\sigma_{\mathrm{breakup}} + \sigma_{1\mathrm{n\text{-}transfer}} = \sigma_{^{7}\mathrm{Li\text{-}production}}$ and the stars in Fig. 3 indicate the sum of the ^{7}Li and α production cross sections. In the present experiment, ^{7}Li, α, and tritium resulting from ^{8}Li breakup can be generated. According to the Ref. [5], most of tritium seem likely to fuse into the target in the present incident energy region and ^{7}Li are possible to capture into the target in the upper half of the experimental region. On the other hand, most of α seem unlikely to fuse into the target in the present incident energy region. Therefore, we can infer that the difference of the semiexperimental DR cross sections and the total breakup / transfer reaction cross sections in Fig. 3 (a) comes from α and ^{7}Li capture.

Figure 3 (b) shows the semiexperimental total reaction cross sections for ^{6,7,8}Li + ^{208}Pb systems. Using Eq. (3), as done in Sec. 2, we extracted the barrier parameter, V_B, with respect to the semiexperimental total reaction cross sections. One of the most interesting things in Table. 4 is about 3MeV reduction of V_B for ^{8}Li + ^{208}Pb system compared with ^{7}Li + ^{208}Pb system and about 4MeV reduction of V_B for the semiexperimental total reaction cross sections compared with that of the complete fusion cross sections for ^{8}Li + ^{208}Pb system. This is somewhat similar to ^{4,6}He + ^{209}Bi systems reported in Ref. [13]. Actually, the reported in Ref. [13] reduction of V_B for ^{6}He + ^{209}Bi system compared with ^{4}He + ^{209}Bi system is about 6MeV. One special feature is that ^{6}He or ^{8}Li consists of α particle and two valence neutrons or ^{7}Li and one valence neutrons, respectively. If the projectile and target nuclei come close on feeling sufficient nuclear force, the valence neutron(s) of the projectile particles react faster than the core nuclei on target nuclei. As a result, we can consider that the reaction processes of ^{6}He and ^{8}Li compared with those of ^{4}He and ^{7}Li take place from farther. This is the rise of flux from the elastic into the reaction channel, which increases σ_R^{exp} and also corresponds to the lowering of the barrier height, which tends to enhance σ_R^{exp}. Thus, we can deduce that the valence neutron(s) play a role as the lowering of the barrier height, V_B.

4 Conclusions

We investigated the relation between the interaction distance and the lowest threshold separation energy of the projectiles. From the point of view of the threshold separation energy, ^{6}Li can be considered more weakly bound projectile than ^{8}Li. But the lithium isotope with the largest interaction distance is not ^{6}Li but ^{8}Li. Although the threshold separation energy is lower, as a result, the interaction distance is not always far.

In the present experiment, ^{7}Li, α, and tritium resulting from ^{8}Li breakup can be generated. We can infer that the difference of the semiexperimental DR cross sections and the total breakup / transfer reaction cross sections comes from α and ^{7}Li capture.

The Coulomb barrier for ^{8}Li + ^{208}Pb system compared with ^{7}Li + ^{208}Pb system are reduced about 3MeV. This is the rise of flux from the elastic into the reaction channel, which tends to enhance σ_R^{exp}. As a result, we can deduce that the valence neutron(s) play a role as the lowering of the barrier height.

Acknowledgments

This research was supported by Basic Science Research Program through the National Research Foundation of Korea (NRF) funded by the Ministry of Education, Science and Technology (2010-0013235).

References

1. W. Y. So *et al.*, Phys. Rev. C **75**, 024610 (2007); *ibid.* **76**, 024613 (2007).
2. T. Udagawa *et al.*, Phys. Rev. C **32**, 124 (1985); T. Udagawa and T. Tamura, *ibid.* **29**, 1922 (1984).
3. S.-W. Hong *et al.*, Nucl. Phys. **A491**, 492 (1989).
4. J. J. Kolata *et al.*, Phys. Rev. C. **65**, 054616 (2002).
5. E. F. Aguilera *et al.*, Phys. Rev. C. **80**, 044605 (2009).
6. G. R. Satchler, Introduction to Nuclear Reactions (Wiley, New York, 1980).
7. R. Bass, Nuclear Reactions with Heavy Ions (Springer-Verlag, New York, 1980).
8. Y. W. Wu *et al.*, Phys. Rev. C. **68**, 044605 (2003).
9. M. Dasgupta *et al.*, Phys. Rev. C **70**, 024606 (2004).
10. C. Y. Wong, Phys. Rev. Lett. **31**, 766 (1973).
11. A. M. Vinodkumar *et al.*, Phys. Rev. C. **80**, 054609 (2009).
12. N. Keeley *et al.*, Nucl. Phys. **A571**, 326 (1994).
13. E. F. Aguilera *et al.*, Phys. Rev. C. **63**, 061603(R) (2001).